

# Oxyhalogen–sulfur chemistry — Kinetics and mechanism of oxidation of methionine by aqueous iodine and acidified iodate

Edward Chikwana, Bradley Davis, Moshood K. Morakinyo, and Reuben H. Simoyi

**Abstract:** The oxidation of methionine (Met) by acidic iodate and aqueous iodine was studied. Though the reaction is a simple two-electron oxidation to give methionine sulfoxide (Met–S=O), the dynamics of the reaction are, however, very complex, characterized by clock reaction characteristics and transient formation of iodine. In excess methionine conditions, the stoichiometry of the reaction was deduced to be  $\text{IO}_3^- + 3\text{Met} \rightarrow \text{I}^- + 3\text{Met-S=O}$ . In excess iodate, the iodide product reacts with iodate to give a final product of molecular iodine and a 2:5 stoichiometry:  $2\text{IO}_3^- + 5\text{Met} + 2\text{H}^+ \rightarrow \text{I}_2 + 5\text{Met-S=O} + \text{H}_2\text{O}$ . The direct reaction of iodine and methionine is slow and mildly autoinhibitory, which explains the transient formation of iodine, even in conditions of excess methionine in which iodine is not a final product. The whole reaction scheme could be simulated by a simple network of 11 reactions.

**Key words:** methionine, organosulfur, iodine, antioxidant, nonlinear dynamics, methionine sulfoxide.

**Résumé :** On a étudié la réaction d'oxydation de la méthionine (Met) par l'ion iodate, en milieu acide et en présence d'iode aqueux. Même si la réaction d'une simple oxydation à deux électrons pour conduire au sulfoxyde de méthionine (Met–S=O), la dynamique de la réaction est toutefois fort complexe ayant les caractéristiques d'une réaction horloge et comportant la formation transitoire d'iode. Dans des conditions où la méthionine est en excès, on a déduit que la stoechiométrie de la réaction est  $\text{IO}_3^- + 3\text{Met} \rightarrow \text{I}^- + 3\text{Met-S=O}$ . Dans des conditions où l'iodate est en excès, l'iodure produit réagit avec l'iodate pour donner de l'iode moléculaire comme produit final avec une stoechiométrie 2:5:  $2\text{IO}_3^- + 5\text{Met} + 2\text{H}^+ \rightarrow \text{I}_2 + 5\text{Met-S=O} + \text{H}_2\text{O}$ . La réaction directe de l'iode avec la méthionine est très lente et donne lieu à une légère autoinhibition qui explique la formation transitoire d'iode, même dans des conditions d'excès de méthionine dans lesquelles l'iode n'est pas un produit final. L'ensemble des réactions peut être simulé par un réseau simple de onze réactions.

**Mots-clés :** méthionine, organosulfuré, iode, antioxydant, dynamique non linéaire, sulfoxyde de méthionine.

[Traduit par la Rédaction]

## Introduction

Methionine is an essential amino acid, obtained only from dietary sources and found mainly in animal protein. In addition to its role as a precursor in protein synthesis, L-methionine participates in a wide range of biochemical reactions, including the production of S-adenosyl methionine, homocysteine, L-cysteine, taurine, and sulfate. It is believed to be the major methyl donor for methylation of DNA, RNA, proteins, and other molecules.<sup>1,2</sup> Methionine is also thought to keep fat from building up in the liver, and it is often included in liver-detoxifying products called lipotropic combinations.<sup>3</sup> These formulations are believed to accelerate the flow of bile and cell-damaging toxins away from the liver.

Depletion of methionine is strongly linked to inhibited growth, apoptotic death, and necrosis of cancerous cells, es-

pecially in combination with chemotherapy.<sup>4</sup> On the other hand, high levels of methionine in the physiological system are associated with several metabolic disorders such as homocystinuria, which is characterized by increased levels of homocysteine in the serum.<sup>5</sup> Homocystine is one of the products of methionine metabolism and its accumulation has been linked to atherosclerosis and arteriosclerosis.<sup>1,5</sup> Atherosclerosis is characterized by the development of lesions within and around blood vessels.<sup>5,6</sup> While atherosclerosis provides the plaque that narrows the artery, arteriosclerosis stiffens the arteries so that they cannot expand with each heart beat to compensate for the blockage caused by plaque formation.<sup>6,7</sup> In most cases of myocardial infarction, both atherosclerosis and arteriosclerosis have been shown to be present.

It has been proposed that methionine residues in proteins serve as an antioxidant defense system for the protection of proteins from oxidation under conditions of oxidative stress.<sup>8,9</sup> Various biological oxidants, such as hydrogen peroxide, hydroxyl radicals, ozone, peroxydinitrite, and hypochlorite, have been shown to mediate the oxidation of methionine.<sup>9,10</sup> Methionine has been shown to be effective in radical scavenging processes, such as those involving reactive nitrogen species, to form methionine sulfoxide and ethylene.<sup>9</sup> In the physiological environment, oxidation of methionine residues to methionine sulfoxide is easily re-

Received 24 October 2008. Accepted 24 December 2008.

Published on the NRC Research Press Web site at [canjchem.nrc.ca](http://canjchem.nrc.ca) on 7 May 2009.

E. Chikwana,<sup>1</sup> B. Davis, M.K. Morakinyo, and R.H. Simoyi.<sup>2</sup>  
Department of Chemistry, Portland State University, Portland,  
OR 97207-0751, USA.

<sup>1</sup>Present address: Department of Chemistry, Franklin College,  
Franklin, IN 46131-2623, USA.

<sup>2</sup>Corresponding author (e-mail: [rsimoyi@pdx.edu](mailto:rsimoyi@pdx.edu)).

**Fig. 1.** Titration results for the oxidation of methionine in excess iodate conditions. The  $x$ -intercept strongly suggest a 1:3 (iodate:methionine) stoichiometric ratio.  $[\text{Met}]_0 = 3.0 \times 10^{-3}$  mol/L,  $[\text{H}^+]_0 = 6 \times 10^{-3}$  mol/L.

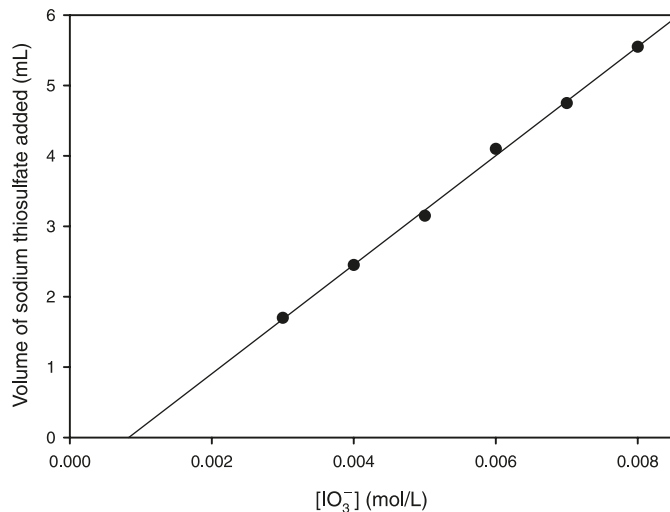
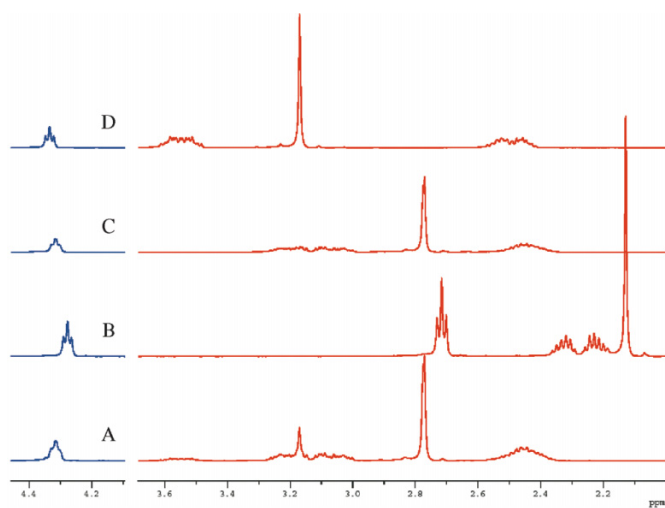


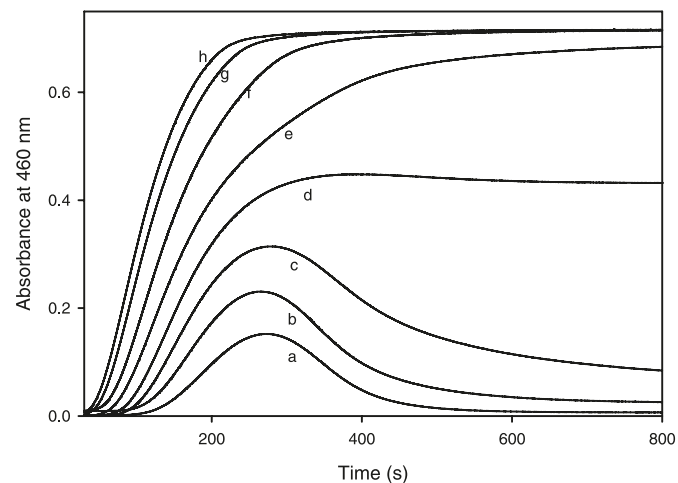
**Fig. 2.** (A) NMR spectrum for the product of the DL-methionine oxidation by acidic iodate/iodine solution showing the  $S$ -methyl peak at 2.79 ppm. (B) Spectrum of DL-methionine shows the peak initially at 2.12 ppm. Spectra for reagent grade methionine sulfoxide (C) and methionine sulfone (D) shows the shifting in the  $S$ -methyl group as expected from the oxidation of the sulfur center. The product solution in this case shows strong similarity to the spectrum of the sulfoxide as predicted from the stoichiometric determination.



versed by the action of the enzyme methionine sulfoxide reductase.<sup>9</sup> Even though methionine has three coordinating centers (O, N, and S), studies have shown that the sulfur center is the most susceptible to oxidative attack.<sup>9,11–13</sup>

The key to understanding the physiological role of methionine requires an understanding of its specialized function, its reactive intermediates, and oxidation products. Even though most of the methionine is believed to be metabolized in the liver via the transmethylation and transsulfuration pathways,<sup>1</sup> alternative pathways cannot be excluded. Its interaction with different oxidants in the physiological

**Fig. 3.** Iodate variation shows transient iodine formation below the stoichiometry (traces a–c). In excess iodate conditions, the final iodine amount reaches a maximum determined by the methionine concentration as shown by traces e–h. The relation between iodate concentration and induction time is also apparent.  $[\text{Met}]_0 = 0.005$  mol/L,  $[\text{H}^+]_0 = 0.02$  mol/L,  $[\text{IO}_3^-]_0 =$  (a) 0.001, (b) 0.00125, (c) 0.0015, (d) 0.00175, (e) 0.002, (f) 0.0025, (g) 0.003, (h) 0.004 mol/L.



system, such as the oxygen radical species, hydrogen peroxide, hypobromous acid, hypochlorous acid, and iodine, can go a long way in providing data on the depletion of excessive dietary methionine in tissues that, unlike the liver, do not contain the complete methionine cycle.

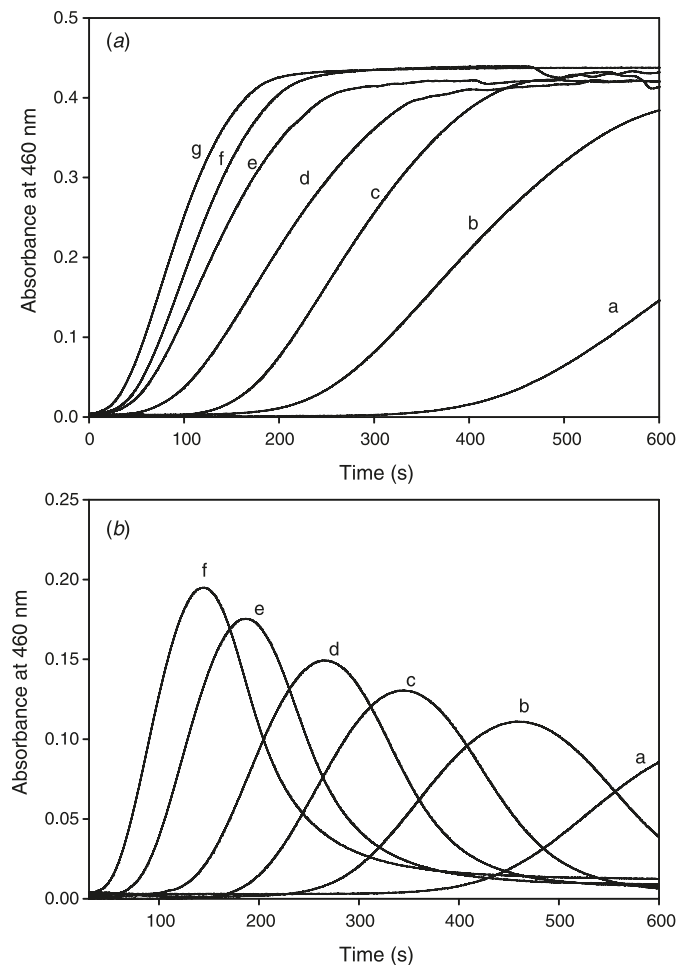
Methionine has also been shown to inhibit *in vivo* thyroid peroxidase (TPO) iodide oxidation and iodination activities.<sup>11,14</sup> Its reaction with iodine is expected to play a major role in its interaction with the thyroid enzymes. Several organosulfur compounds are well-known goitrogens whose actions are based on their ability to abstract the active iodine cation from the thyroid, thereby reducing its hyperactivity.<sup>15–19</sup> We report, in this manuscript, on a detailed kinetics and mechanistic study of the oxidation by iodate/iodine of DL-methionine. This simple oxidation reaction was surprisingly complex, characterized by nonlinear exotic kinetics behavior.

## Experimental

### Materials

Iodine, potassium iodide (Sigma-Aldrich), sodium perchlorate (98%) (Acros Organics), potassium iodate, DL-methionine (99%), DL-methionine sulfone (99%), DL-methionine sulfoxide, perchloric acid (72%), soluble starch, sodium thiosulfate, and hydrochloric acid (Fisher Scientific) were used without further purification. The concentration of iodine was determined by standardization against thiosulfate with starch as the indicator. Spectrophotometry was also utilized by measuring iodine absorbance at its isosbestic point with triiodide at 460 nm where the extinction coefficient had been deduced to be  $770 \text{ (mol/L)}^{-1} \text{ cm}^{-1}$ . This standardization was carried out before each series of kinetics experiments due to the volatile nature of iodine. Methionine solutions were prepared just before use and not kept for more than

**Fig. 4.** (a) The effect of varying acid concentrations for reactions run in excess iodate. Acid is not a reactant in the reaction but strongly catalyzes the reaction by reducing the induction period.  $[\text{Met}]_0 = 0.003 \text{ mol/L}$ ,  $[\text{IO}_3^-]_0 = 0.03 \text{ mol/L}$ ,  $[\text{H}^+]_0 =$  (a) 0.003, (b) 0.004, (c) 0.0045, (d) 0.005, (e) 0.006, (f) 0.007, (g) 0.008 mol/L. (b) The effect of acid variation in excess methionine. The effect of increasing acid can be seen in the form of a shorter induction period and a higher maximum transient iodine concentration.  $[\text{Met}]_0 = 0.005 \text{ mol/L}$ ,  $[\text{IO}_3^-]_0 = 0.001 \text{ mol/L}$ ,  $[\text{H}^+]_0 =$  (a) 0.0125, (b) 0.015, (c) 0.0175, (d) 0.02, (e) 0.025, (f) 0.03 mol/L.



24 h. All solutions were prepared using distilled water from a Barnstead Sybron Corporation water purification unit. Inductively coupled plasma mass spectrometry (ICPMS) was used to show that our reaction medium did not contain enough copper ions to affect the overall reaction kinetics and mechanism.<sup>20</sup>

## Methods

All experiments were carried out at  $25.0 \pm 0.1 \text{ }^\circ\text{C}$  and with a constant ionic strength of  $1.0 \text{ mol/L}$  ( $\text{NaClO}_4$ ). Methionine, sodium perchlorate, and perchloric acid solutions were mixed in one vessel and iodate (or iodine) solutions in another. Kinetics measurements for the slower reactions and spectrophotometric determinations were performed on a PerkinElmer Lambda 25 UV-vis Spectrophotometer. The faster reactions, especially those involving iodine oxidations were monitored on a Hi-Tech Scientific SF-61 stopped-flow spec-

**Fig. 5.** Absorbance traces for methionine variation in its oxidation by iodate. Initially, the final iodine absorbances increase (a–d) but as the stoichiometric point is approached they start to decrease and show transient iodine formation (e).  $[\text{IO}_3^-]_0 = 0.003 \text{ mol/L}$ ,  $[\text{H}^+]_0 = 0.0045 \text{ mol/L}$ ,  $[\text{Met}]_0 =$  (a) 0.003, (b) 0.004, (c) 0.005, (d) 0.006, (e) 0.007 mol/L.

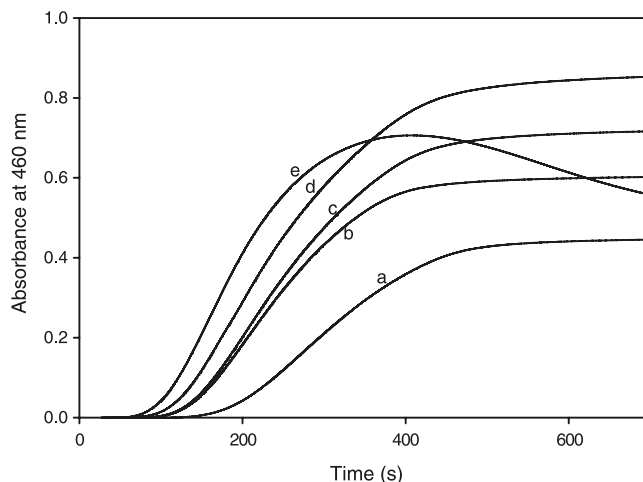
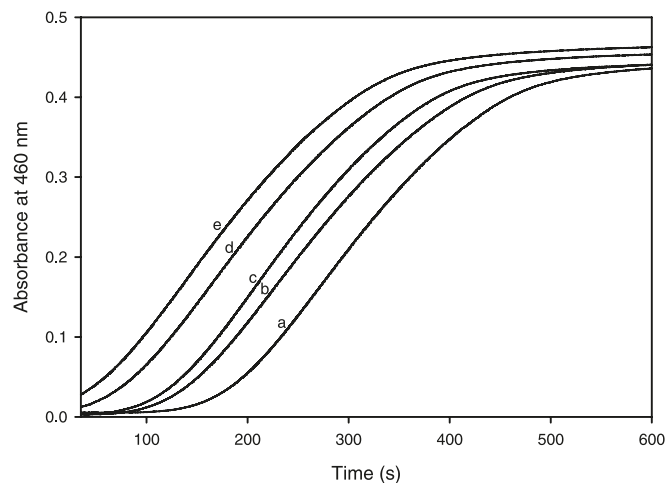


**Fig. 6.** Iodide effect on the iodate oxidation of methionine. The effect of iodide can be seen on the reduced induction period and increased final absorbance of iodine as iodide concentration is increased.  $[\text{Met}]_0 = 0.003 \text{ mol/L}$ ,  $[\text{H}^+] = 0.0045 \text{ mol/L}$ ,  $[\text{IO}_3^-] = 0.0275 \text{ mol/L}$ ,  $[\text{I}^-] =$  (a) no iodide, (b)  $6 \times 10^{-6}$ , (c)  $9 \times 10^{-6}$ , (d)  $5 \times 10^{-5}$ , (e)  $1 \times 10^{-4} \text{ mol/L}$ .

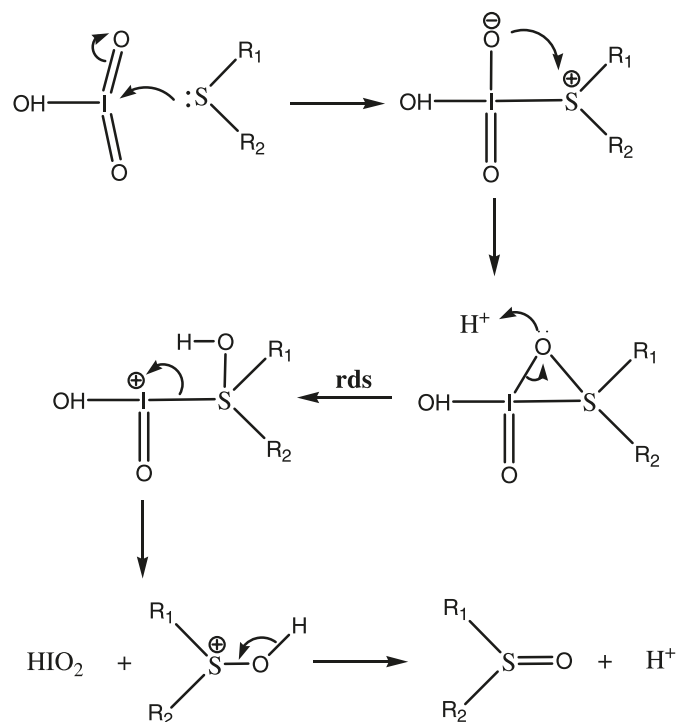


trophotometer as well as on a Hi-Tech Scientific SF-DX2 double-mixing stopped-flow spectrophotometer.

## Stoichiometric determinations

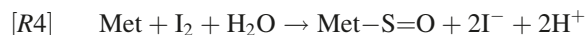
The stoichiometry for the methionine- $\text{IO}_3^-$  reaction was determined both in excess iodate and excess methionine conditions. In excess iodate the total excess oxidizing power was determined by titration. Excess acidified iodide was added to the reaction solution and the released iodine was titrated against standard thiosulfate. Spectrophotometric measurements were also used to determine the amount of iodine formed in excess iodate by its absorbance at 460 nm. In the  $\text{I}_2$ -methionine reaction, the stoichiometry was determined by titrating standardized iodine solution from a bu-



**Scheme 1.** Mechanism of reaction of methionine with iodic acid.

Essentially, stoichiometry eq. [R3] is a linear combination of stoichiometry eqs. [R1] and [R2]: [R1] + 5[R2]. Iodine produced in stoichiometry eq. [R1] is consumed by the excess iodate to produce iodine, and the end of reaction is determined by a complete consumption of iodide for as long as there is still excess iodate to fuel the Dushman reaction, eq. [R1]. Initially there is an increase in the amount of iodine produced as the iodate to substrate ratio,  $R = [\text{IO}_3^-]_0/[\text{Met}]_0$ , is increased from 0.333 (stoichiometry eq. [R2]), until a saturation point is reached where the methionine becomes limiting at a ratio of 0.400. In this short range of ratios, the final iodine amount was reproducibly determined spectrophotometrically to be 0.2 times the amount of methionine used as predicted by stoichiometry eq. [R3].

The direct reaction of methionine with iodine was rapid enough for the stoichiometry to be determined by direct titration of an iodine solution with methionine and vice-versa. The detection of the end point was aided by the starch indicator and the stoichiometry was determined to be



Stoichiometry eq. [R4] could also be obtained spectrophotometrically in excess iodine conditions by observing the absorbance of the excess iodine at 460 nm (at the end of the reaction).

### Confirmation of products

The two major products that could possibly be obtained from the oxyhalogen oxidation of the sulfur center in methionine are the sulfoxide and the sulfone. Due to the lack of  $\text{BaSO}_4$  precipitation, there was no evidence to suggest further

oxidation resulting in cleavage to the C-S bond. Proton NMR spectroscopy was used to confirm the products as predicted from the stoichiometry. In Fig. 2, spectrum A is of the product of reaction between acidic iodate and methionine. Spectrum B is pure DL-methionine, which shows the expected strong singlet for the S-methyl group at 2.12 ppm. These protons appear as a singlet due to the presence of the sulfur, which acts as a shield from the splitting effects of the other protons on adjacent carbon atoms. Spectrum C shown is of reagent grade DL-methionine sulfoxide, showing a downfield shift of the methyl protons (2.79 ppm) due to the presence of the oxygen on the sulfur center. Addition of another oxygen to form the sulfone results in a further downfield shift of these protons to 3.20 ppm. Spectrum D is reagent grade methionine sulfone. Spectrum A, the reaction product, is similar to the spectrum for the reagent grade sulfoxide (C). Solutions to obtain spectra B-D were prepared in neutral conditions while DCl was used to acidify the solution used to obtain spectrum A. The difference in pH between these solutions accounts for the small difference between spectra A and C. The spectrum of oxidation of methionine by acidified iodate shows that there is a small amount of sulfone formed as a minor product, but this could not be detected iodometrically due to the oxidation of iodide by the sulfone to iodine and the sulfoxide. To further confirm the sulfoxide as the major product, reagent grade sulfoxide was mixed with acidified iodate solution and no further reaction was observed.

### Reaction dynamics

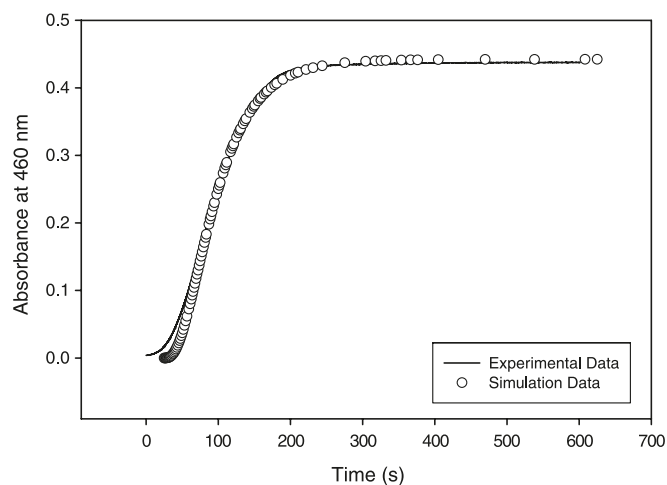
The reaction exhibited clock behavior<sup>22</sup> with transient iodine formation. Figure 3 shows both aspects of this dynamical behavior. When the oxidant-to-reductant ratio,  $R = [\text{IO}_3^-]_0/[\text{Met}]_0$ , is less than 0.333, no iodine is expected to be formed at the end of the reaction as predicted by stoichiometry eq. [R2]. Traces a-c in Fig. 3 are derived from reaction solutions in which  $R < 0.333$ , but, however, show transient iodine formation, which is an indication of the dominance of the reactions that form iodine over those that consume it during the initial stages of the reaction. As the reaction proceeds, iodine consumption reactions later become dominant. Clock reaction characteristics, in which there is an initial quiescent period followed by formation of iodine, are also exhibited for all values of  $R$ , as shown by traces a-h (Fig. 3). In stoichiometric excess of oxidant, which gives stoichiometry eq. [R3], i.e.,  $R \geq 0.333$ , the final iodine formation is determined by the concentration of methionine. When  $R > 0.4$ , however, the amount of iodine formed becomes invariant to further increases in iodate concentrations. The increase in final iodine concentration between traces d and e (Fig. 3) is justified based on the fact that stoichiometry eq. [R3] is a step wise linear combination of eqs. [R1] and [R2].

Figure 3 also shows that as the iodate concentration is increased, the rate of iodine formation increases while the quiescent time before iodine formation commences (induction period), decreases.<sup>23</sup> Formation of iodine, in all traces (Fig. 3), is not sharp, but gradual. Thus the induction period was estimated to be the point where rapid formation of iodine commenced.

Figure 4a shows that not only does an increase in acid decrease the induction period, but it also increases the rate of

**Table 1.** Iodate–Iodine–Methionine reaction network.

Number	Reaction	$K_f$ ; $k_r$
M1	$\text{IO}_3^- + \text{I}^- + 2\text{H}^+ \rightleftharpoons \text{HIO}_2 + \text{HOI}$	2.8; $1.44 \times 10^3$
M2	$\text{HIO}_2 + \text{I}^- + \text{H}^+ \rightleftharpoons 2\text{HOI}$	$2.1 \times 10^8$ ; 90
M3	$\text{HOI} + \text{I}^- + \text{H}^+ \rightleftharpoons \text{I}_2 + \text{H}_2\text{O}$	$3.1 \times 10^{12}$ ; 2.2
M4	$\text{IO}_3^- + \text{HOI} + \text{H}^+ \rightleftharpoons 2\text{HIO}_2$	$8.6 \times 10^2$ ; 2.00
M5	$\text{I}_2 + \text{I}^- \rightleftharpoons \text{I}_3^-$	$6.2 \times 10^9$ ; $8.5 \times 10^6$
M6	$\text{IO}_3^- + \text{H}^+ \rightleftharpoons \text{HIO}_3$	$5.0 \times 10^9$ ; $1.25 \times 10^9$
M7	$\text{HIO}_3 + \text{Met} + \text{H}^+ \rightarrow \text{HIO}_2 + \text{Met-SO} + \text{H}^+$	50
M8	$\text{HIO}_2 + \text{Met} \rightarrow \text{HOI} + \text{Met-SO}$	125
M9	$\text{HOI} + \text{Met} \rightarrow \text{Met-SO} + \text{I}^- + \text{H}^+$	165
M10	$\text{I}_2 + \text{Met} + \text{H}_2\text{O} \rightarrow \text{Met-SO} + 2\text{H}^+ + 2\text{I}^-$	72
M11	$\text{I}_3^- + \text{Met} + \text{H}_2\text{O} \rightarrow \text{Met-SO} + 2\text{H}^+ + 3\text{I}^-$	16

**Fig. 9.** Computer modeling: traces showing the simulated results (circles) and the experimental data (solid line) for trace g shown in Fig. 4a.  $[\text{Met}]_0 = 0.003 \text{ mol/L}$ ,  $[\text{IO}_3^-]_0 = 0.03 \text{ mol/L}$ ,  $[\text{H}^+] = 0.008 \text{ mol/L}$ .

formation of iodine. The catalytic effect of acid on the Dushman<sup>24–27</sup> reaction (eq. [R1]) is responsible for the increase in rate of formation of iodine in conditions where  $R > 0.4$ . Since the final amount of iodine does not change with an increase in acid, acid influences only the overall rate of formation of iodine, which in turn affects the induction period. The effect of acid for low  $R$  values ( $R < 0.33$ ), however, is more complex as shown in Fig. 4b. Figure 4b shows traces in excess methionine conditions where no final iodine accumulation is expected. As the acid is increased from a to f (Fig. 4b), the induction period is shortened while the maximum amount of transient iodine is increased. This indicates acid catalysis in formation of iodine, resulting in rapid accumulation of iodine and shorter induction periods as acid concentrations are increased. Higher acid traces in Fig. 4b also show a narrower “excursion” indicating that an increase in acid also increases the rate of consumption of iodine. Given that the general shape of the traces is not symmetrical, it would also appear that acid catalyzes the formation of iodine to a greater extent than it catalyzes its consumption.

The oxidant-to-reductant ratio,  $R$ , plays an important role in determining the dynamics of the reaction as can be seen in Fig. 5, which shows the effect of progressively increasing the methionine concentration at constant iodate and acid

concentration. As  $R$  is reduced from a–d (Fig. 5), the final iodine amount increases to a final concentration that is determined by stoichiometry eq. [R3]. As reaction stoichiometry eq. [R2] is approached, the monotonic formation of iodine gives way to transient formation of iodine as shown in trace e (Fig. 5).

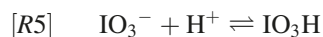
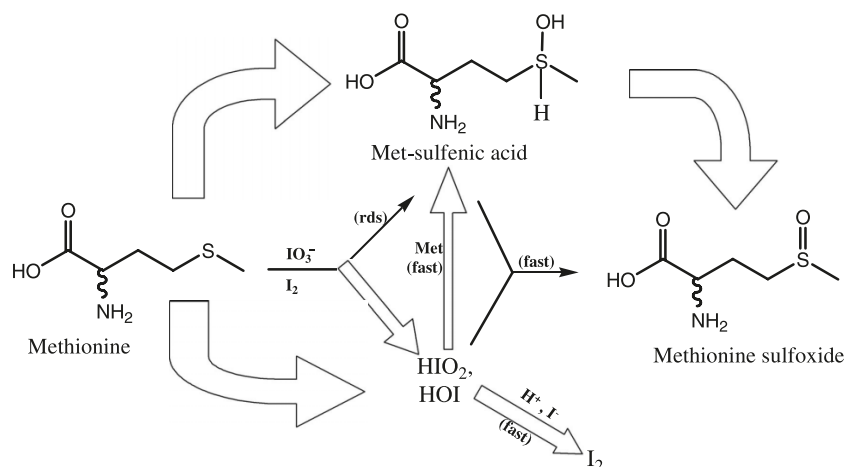
In excess oxidant conditions, the effect of iodide can easily be seen by the increase in final iodine concentration. This is expected in conditions where  $R > 0.4$ , in which the iodide ions initially added to the reaction mixture combine with those produced by the reaction in eq. [R2] to fuel the Dushman reaction,<sup>24,26</sup> eq. [R1]. This is clearly evident in Fig. 6 where an increase in iodide concentrations increases the final iodine concentration as well as reducing the induction time.

The direct reaction of iodine and methionine plays a crucial role in this mechanism. The rate at which iodine oxidizes methionine determines whether methionine can coexist with iodine. If this reaction is fast, then final iodine formation would mean that all the methionine has been consumed. Figure 7a shows the iodine consumption of methionine in high excess of methionine. Despite this high excess, no pseudo-first-order kinetics are observed, indicating that this is not a simple electrophilic attack of iodine on the thioether group. There is a linear dependence between the initial rate of reaction with both methionine and iodine concentrations. Figure 7b shows the methionine dependence. Figure 8a shows that iodide is inhibitory to the oxidation of methionine by iodine. Figure 8b shows that there is an inverse dependence relationship between the initial rate of reaction and iodide concentrations. Iodide is a product of the iodine–methionine reaction, and thus its effect is autoinhibitory. This explains why no pseudo-first-order kinetics were observed in the data shown in Fig. 7a.

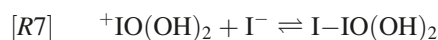
## Mechanism

The bulk of iodate-based oxidations are borne by the reactive oxyiodine species  $\text{HIO}_2$ ,  $\text{IO}_2$ , and  $\text{HOI}$  as well as molecular iodine,  $\text{I}_2$ . These species can be generated in acidic iodate conditions, and the rate of iodate oxidations are usually controlled by the rate at which these reactive species are generated.<sup>28,29</sup> There is some debate as to the exact initiation sequence of iodate oxidations, but a nucleophilic attack on a protonated iodate species (see reaction eq. [R7]) appears to be the most widely accepted initiation to produce iodous and hypoiodous acids.

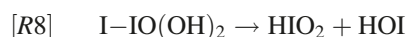
**Scheme 2.** Schematic representation of all possible reactions, intermediates, and products in the oxidation of methionine by acidic iodate and aqueous iodine.



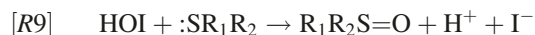
Investigators of the Briggs–Rauscher<sup>30,31</sup> and Bray–Liebhafsky<sup>25,32</sup> reactions have suggested that this nucleophilic species is the trace amount of iodide ions that are contained in normal iodate solutions.



The  $\text{H}_2\text{I}_2\text{O}_3$  species formed in eq. [R7] can then break down in a rate-determining step to produce the reactive species,  $\text{HIO}_2$  and  $\text{HOI}$ .<sup>29</sup>



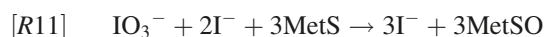
$\text{HOI}$  is extremely reactive as an oxidizing species, and will rapidly react with the substrate, methionine, to produce iodide and the oxidation product, methionine sulfoxide.



The iodide produced in eq. [R9] feeds back into reaction eq. [R7] to facilitate further oxidation of the reactive species. While we may accept iodic acid as a viable oxidant, it, however, rapidly reacts with iodide to produce more hypoiodous acid:



Addition of the reactions leading to the oxidation of methionine in the initial stages shows that the reaction's initial activity is the build-up of iodide, which is autocatalytically produced in these early stages of the reaction of eqs. [R5] + [R6] + [R7] + [R8] + 3[R9] + [R10];



The iodide material balance for the initial stages suggests a mechanism that is based on cubic autocatalysis in iodide.

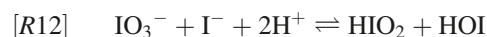
There are, however, two major flaws with the eqs. [R5]–[R10] sequence. The first flaw is from pure mass action

kinetics. The expected iodide concentrations, which exist in these iodate solutions, should be approximately  $5.0 \times 10^{-7}$  mol/L. Assuming eqs. [R9] and [R10] are relatively rapid, one can utilize reaction eq. [R8] to determine the rate of formation of iodide and subsequently the rate of oxidation of methionine. A simple integration gives a sigmoidal curve for iodide generation. Literature values give the composite forward rate constant of reaction eq. [R8] as  $2.2$  (mol/L)<sup>-3</sup> s<sup>-1</sup>. Using these values, one generates a very slow rate of iodide formation and subsequent rate of reaction, giving reaction times in the order of hours instead of the observed 2–10 min. This suggests that iodide formation is not solely through the composite reaction eq. [R11]. The next flaw arises from the effect of iodide observed in Fig. 6. With cubic autocatalysis, as profiled in reaction eq. [R11], addition of minute amounts of iodide should result in a greatly enhanced rate of reaction. Figure 6 shows that, while iodide is catalytic, it is not as strong as would have been expected from an autocatalyst.

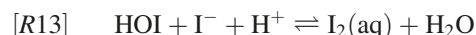
It appears then, that initial formation of iodide should be derived from the substrate itself acting as a nucleophile on either the iodic acid or the protonated iodic acid. Both scenarios would produce kinetically indistinguishable reaction profiles and mechanisms. In Scheme 1, methionine is represented as  $\text{R}_1\text{SR}_2$ .

The iodic acid produced in Scheme 1 can be further reduced successively by methionine to hypoiodous acid and iodide. Reaction eq. [R9] is a rapid oxygen transfer reaction, and thus, the overall rate of reaction should be the rate of formation of  $\text{HOI}$ .

Accumulation of iodide will then transfer the rate of reaction to standard Dushman reaction kinetics with the composite rate-determining step eq. [R12]:



Iodine is formed from the reverse of its hydrolysis reaction:



Through relaxation spectroscopy, reaction eq. [R13] is known to be very rapid and acid-catalyzed.<sup>33</sup> Basic condi-

tions catalyze and support the hydrolysis reaction. Our experiments, however, were carried out in acidic conditions since iodate is essentially inert in basic environments. A summary of all possible reactions, intermediates, and products in the oxidation of methionine by acidic iodate and its oxidative derivatives is shown in Scheme 2.

### The methionine–iodine reaction

The direct reaction of methionine with aqueous iodine is very important in determining the overall global dynamics observed with respect to iodine formation. Transient iodine formation, as observed in Fig. 4*b*, is derived from the coupling of the reaction that forms iodine, eq. [R13],<sup>33</sup> with those that consume iodine. If the methionine–iodine reaction is extremely rapid (e.g., diffusion controlled), no transient iodine formation would be observed and the end of the induction period would be very sharp, and would signify complete consumption of methionine. The nonlinear kinetics observed indicate that the reactions involved in the formation and consumption of iodine are comparable in magnitude and each set asserts itself based on the availability of the relevant reagents and mass action kinetics.

The reaction commences with an electrophilic attack by aqueous iodine on the electron-rich sulfur center of methionine:



followed by the standard hydrolysis:



Addition of eqs. [R14] and [R15] gives the 1:1 experimentally observed stoichiometry for this reaction. Initial rate data, before accumulation of iodide, was used to evaluate  $k_{14} = 72 \pm 1.4 \text{ (mol/L)}^{-1} \text{ s}^{-1}$ .

Although the reaction is autoinhibitory, the autoinhibition is not as strong as the one observed with the iodine–thiocyanate<sup>34,35</sup> and iodine–thiourea reactions.<sup>36</sup> In these systems, it was assumed that iodine reacts with the product, iodide, to produce an inert product, triiodide:



If one assumes that the triiodide anion is inert, then the following rate law emerges:

$$[\text{1}] \quad \left| \frac{1}{\text{Rate}} \right| = \frac{1}{k_{14}[\text{Met}]_0[\text{I}_2]_0} (1 + K_{\text{eq}}[\text{I}^-])$$

A plot of the inverse of the rate versus iodide concentrations on the basis of eq. [1] should give a straight line, which should allow for the calculation of  $k_{14}$  and a confirmation of the well known value of  $K_{\text{eq}} = 770 \text{ (mol/L)}^{-1}$ . This plot is shown in Fig. 8*b* where the data gave a value of  $k_{14}$  that was much lower than that derived from initial rate data, and also gave a much lower  $K_{\text{eq}}$  value that was an order of magnitude lower than the literature value.<sup>37</sup> This suggests that  $\text{I}_3^-$  is not inert, and that the autoinhibition observed is derived from the sluggish kinetics obtained with  $\text{I}_3^-$  when it predominates in concentrations as iodide accumulates.



Combining reaction eqs. [R14] and [R17] gives a rate law of the form

$$[\text{2}] \quad \text{Rate} = \frac{[\text{Met}]_0[\text{I}_2]_0}{1 + K_{\text{eq}}[\text{I}^-]} [k_{14} + k_{17}K_{\text{eq}}[\text{I}^-]]$$

In the initial stages, before iodide accumulates, rate law eq. [2] simplifies to a simple bimolecular rate law. In the limit of high initial iodide concentrations, in which one can assume constant iodide concentrations, an upper limit rate constant for  $k_{17}$  was derived as  $16.0 \text{ (mol/L)}^{-1} \text{ s}^{-1}$ .

### Computer simulation

The reaction scheme was modeled using the Kintecus software generated by James Ianni.<sup>41</sup> The full mechanism, which takes into account the formation and consumption of iodine, is shown in Table 1. It is a very simple mechanism made up of 11 reactions with the most important reactions being M1 and M7 (Table 1), which are responsible for initiating the reaction. Since iodate oxidations only proceed at reasonable rates in highly acidic media, the simulations could be simplified by assuming that acid concentrations were buffered throughout the duration of the reaction. By using a constant acid concentration, reactions M2–M4 and M7 (Table 1) could be reduced to the simpler bimolecular kinetics. Reactions M1–M4 (Table 1) are the standard oxy-iodine reactions whose rate constants are well-known and were derived from literature.<sup>24–27</sup> These were not altered during the modeling exercises. Reaction M5 (Table 1) was studied by laser-Raman techniques and the forward and reverse rate constants and subsequent equilibrium constant were also derived from literature and also not varied.<sup>37,38</sup> Reaction M6 (Table 1) is a rapid protolytic process in which the only relevant parameter was the assumed  $K_a$  of iodic acid. Literature reports a wide range of values for this  $K_a$ .<sup>39</sup> The  $K_a$  value is apparently heavily dependent on the reaction medium, especially acid concentrations.<sup>29</sup> Elegant experimental work done by Naidich and Ricci<sup>40</sup> in 1939 established that concentrations of iodic acid become significant in acidic iodate solutions at a pH of less than 2.00. All our reactions were run at pH conditions lower than this value. The final adopted value of 0.400 was extrapolated from the barium iodate solubility data of Naidichi and Ricci.<sup>40</sup> The simulations were insensitive to the adopted values of the forward and reverse rate constants for M6 (Table 1) for as long as they were both rapid and linked by  $K_a$ . More realistic diffusion-controlled rate constants for M6 (Table 1) stiffened the simulations considerably and slowed the calculations but without affecting the resulting simulations. Reactions M7–M9 (Table 1) represent the initiation reactions in the absence of initially added iodide. Reactions M8 and M9 (Table 1) are not important in determining the observed reaction dynamics for as long as they are faster than M7 (Table 1). Rate constants for reactions M10 and M11 (Table 1) were determined from this study. Effectively, since half of the reactions' parameters were obtained from literature values, the only parameters that could be altered for best fit to the data were  $K_a$  for iodic acid and  $k_{M7}$ . Figure 9 shows that this simple mechanism gave a reasonably good fit of the experimental data for the case involving excess io-

date concentrations, resulting in a monotonic formation of iodine. The transient iodine formation traces (Figs. 3 and 4b) were more difficult to reproduce with this abbreviated mechanism. It was easier to fit the initial formation of iodine but much more difficult to fit its consumption, even though the model could easily reproduce the trivial iodine consumption traces shown in Fig. 7a. The inability to correctly simulate Figs. 3 and 4b lay in our inability to correctly ascribe the correct activity of aqueous iodine in these highly acidic solutions. Literature does not contain reliable data on these solutions, especially when spiked with iodide.

## Conclusion

Our short study has shown that iodine oxidizes the simple biologically important thioether, methionine, to just the sulf-oxide. Organosulfur compounds are the most effective goitrogenics available, and their reaction rate and mechanism with iodine would be a significant physiological interaction.

## Acknowledgements

This work was supported by grant number CHE 0614924 from the National Science Foundation.

## References

- Boers, G. H.; Smals, A. G.; Trihbels, J. F.; Leermakers, A. I.; Kloppenborg, P. W. *J. Clin. Invest.* **1983**, *72*, 1971. doi:10.1172/JCI111161. PMID:6643682.
- Epner, D. E. *J. Am. Coll. Nutr.* **2001**, *20*, 443S. PMID:11603655.
- Finkelstein, J. D.; Martin, J. J. *J. Biol. Chem.* **1986**, *261*, 1582. PMID:3080429.
- Yang, Z.; Wang, J.; Yoshioka, T.; Li, B.; Lu, Q.; Li, S.; Sun, X.; Tan, Y.; Yagi, S.; Frenkel, E. P.; Hoffman, R. M. *Clin. Cancer Res.* **2004**, *10*, 2131. doi:10.1158/1078-0432.CCR-03-0068. PMID:15041734.
- Wilcken, D. E.; Wilcken, B. *J. Clin. Invest.* **1976**, *57*, 1079. doi:10.1172/JCI108350. PMID:947949.
- Wasan, K. M.; Cassidy, S. M.; Kennedy, A. L.; Peteherych, K. D. *Atherosclerosis: Experimental Methods and Protocols*; Humana Press: Clifton, NJ, 1995; pp 27–35.
- Zieman, S. J.; Melenovsky, V.; Kass, D. A. *Arterioscler. Thromb. Vasc. Biol.* **2005**, *25*, 932. doi:10.1161/01.ATV.0000160548.78317.29. PMID:15731494.
- Moskovitz, J.; Berlett, B. S.; Poston, J. M.; Stadtman, E. R. *Proc. Natl. Acad. Sci. U.S.A.* **1997**, *94*, 9585. doi:10.1073/pnas.94.18.9585. PMID:9275166.
- Stadtman, E. R.; Moskovitz, J.; Berlett, B. S.; Levine, R. L. *Mol. Cell. Biochem.* **2002**, *234–235*, 3. doi:10.1023/A:1015916831583.
- Moskovitz, J.; Berlett, B. S.; Poston, J. M.; Stadtman, E. R. *Proc. Natl. Acad. Sci. U.S.A.* **1997**, *94*, 9585. doi:10.1073/pnas.94.18.9585. PMID:9275166.
- Carvalho, D. P.; Ferreira, A. C. F.; Coelho, S. M.; Moraes, J. M.; Camacho, M. A. S.; Rosenthal, D. *Braz. J. Med. Biol. Res.* **2000**, *33*, 355. PMID:10719389.
- Levine, R.; Mosoni, L.; Berlett, B.; Stadtman, E. *Proc. Natl. Acad. Sci. U.S.A.* **1996**, *93*, 15036. doi:10.1073/pnas.93.26.15036. PMID:8986759.
- Meenakshisundaram, S.; Vinothini, R. *Croat. Chem. Acta* **2003**, *76*, 75.
- Sato, K.; Robbins, J. *Endocrinology* **1981**, *109*, 844. PMID:6790265.
- Miller, W. H.; Roblin, R. O.; Astwood, E. B. *J. Am. Chem. Soc.* **1945**, *67*, 2201. doi:10.1021/ja01228a043.
- Doniach, I. *Monogr. Neoplast. Dis. Var. Sites* **1970**, *6*, 73. PMID:4950336.
- Lindsay, R. H.; Hulsey, B. S.; Aboul-Enein, H. Y. *Biochem. Pharmacol.* **1975**, *24*, 463. doi:10.1016/0006-2952(75)90129-X. PMID:46147.
- Kabadi, U.; Cech, R. *Thyroidology* **1994**, *6*, 87. PMID:7545000.
- Oren, R.; Dotan, I.; Papa, M.; Marravi, Y.; Aeed, H.; Barg, J.; Zeidel, L.; Bruck, R.; Halpern, Z. *Hepatology* **1996**, *24*, 419. doi:10.1002/hep.510240221. PMID:8690414.
- Darkwa, J.; Olojo, R.; Chikwana, E.; Simoyi, R. H. *J. Phys. Chem. A* **2004**, *108*, 5576. doi:10.1021/jp049748k.
- Chikwana, E.; Otoikhian, A.; Simoyi, R. H. *J. Phys. Chem. A* **2004**, *108*, 11591. doi:10.1021/jp045897r.
- Oliveira, A. P.; Faria, R. B. *J. Am. Chem. Soc.* **2005**, *127*, 18022. doi:10.1021/ja0570537. PMID:16366551.
- Chanakira, A.; Chikwana, E.; Peyton, D.; Simoyi, R. *Can. J. Chem.* **2006**, *84*, 49. doi:10.1139/v05-263.
- Liebhafsky, H. A.; Roe, G. M. *Int. J. Chem. Kinet.* **1979**, *11*, 693. doi:10.1002/kin.550110703.
- Kolaranic, L.; Schmitz, G. *J. Chem. Soc., Faraday Trans.* **1992**, *88*, 2343. doi:10.1039/ft9928802343.
- Schmitz, G. *Phys. Chem. Chem. Phys.* **1999**, *1*, 1909. doi:10.1039/a809291e.
- Schmitz, G. *Phys. Chem. Chem. Phys.* **2000**, *2*, 4041. doi:10.1039/b003606o.
- Mambo, E.; Simoyi, R. H. *J. Phys. Chem.* **1993**, *97*, 13662. doi:10.1021/j100153a039.
- Xie, Y.; McDonald, M. R.; Margerum, D. W. *Inorg. Chem.* **1999**, *38*, 3938. doi:10.1021/ic9807442.
- Tiktonova, L. P.; Kovalenko, A. S.; Labunskaya, I. F.; Ivashchenko, T. S. *Teoreticheskaya I Eksperimentalnaya Khimiya* **1991**, *27*, 737.
- Lalitha, P. V. N.; Ramaswamy, R. *Collect. Czech. Chem. Commun.* **1992**, *57*, 2235. doi:10.1135/cccc19922235.
- Agreda B, J. A.; Field, R. J.; Lyons, N. J. *J. Phys. Chem. A* **2000**, *104*, 5269. doi:10.1021/jp000271w.
- Eigen, M.; Kustin, K. *J. Am. Chem. Soc.* **1962**, *84*, 1355. doi:10.1021/ja00867a005.
- Simoyi, R. H.; Manyonda, M.; Masere, J.; Mtambo, M.; Ncube, I.; Patel, H.; Epstein, I. R.; Kustin, K. *J. Phys. Chem.* **1991**, *95*, 770. doi:10.1021/j100155a052.
- Simoyi, R. H.; Epstein, I. R.; Kustin, K. *J. Phys. Chem.* **1989**, *93*, 2792. doi:10.1021/j100344a019.
- Rabai, G.; Beck, M. T. *J. Chem. Soc. Dalton Trans.* **1985**, 1669. doi:10.1039/dt9850001669.
- Turner, D. H.; Flynn, G. W.; Sutin, N.; Beitz, J. V. *J. Am. Chem. Soc.* **1972**, *94*, 1554. doi:10.1021/ja00760a020.
- Ruasse, M. F.; Aubard, J.; Galland, B.; Adenir, A. *J. Phys. Chem.* **1986**, *90*, 4382. doi:10.1021/j100409a034.
- Kraus, C. A.; Parker, H. C. *J. Am. Chem. Soc.* **1922**, *44*, 2429. doi:10.1021/ja01432a011.
- Naidich, S.; Ricci, J. E. *J. Am. Chem. Soc.* **1939**, *61*, 3268. doi:10.1021/ja01267a010.
- Ianni, J. C. Kintecus, Windows Version 3.95, 2008, <http://www.kintecus.com/>.